Experimental Investigation of Subsonic Turbulent Separated Boundary Layers on an Airfoil

H.C. Seetharam* and W.H. Wentz Jr.†
Wichita State University, Wichita, Kan.

Detailed measurements of flowfields associated with low speed turbulent boundary layers have been made for the 17% thick GA(W)-1 airfoil section at nominal angles of attack of 10, 14, and 18 deg; Reynolds number 2.2×10^6; and Mach number 0.13. The data include extensive pressure and velocity surveys of the pre- and post-separated regions on the airfoil and the associated wake. Integrated boundary-layer characteristics including regions of separation on the airfoil are also presented.

The results indicate steep gradients of displacement thickness, momentum thickness, shape factor, and the separation streamline from the point of separation to the trailing edge of the airfoil. The present tests reveal that the region of flow reversal terminates within a suprisingly short distance of less than 20% chord downstream from the trailing edge for the test range of angle of attack.

Nomenclature

c = wing chord
c_{p_s} = static pressure coefficient, $(p_s - p_\infty/q_\infty)$
c_{p_T} = total pressure coefficient, $(p_T - p_\infty/q_\infty)$
H = shape factor (δ^*/δ^{**})
p_s = local static pressure
p_T = local total pressure
p_∞ = freestream static pressure
q_∞ = freestream dynamic pressure
RN = Reynolds number based upon wing chord
U = velocity at the edge of the boundary layer, nondimensionalized with respect to freestream velocity
u = local velocity, nondimensionalized with respect to freestream velocity
u_x = component of local velocity in the freestream direction, nondimensionalized with respect to freestream velocity
x = streamwise coordinate
y = spanwise coordinate
z = vertical coordinate
α = angle of attack, deg
δ = boundary layer thickness
δ^* = boundary layer displacement thickness, $\int_0^\delta [1-(u/U)]\,dz$
δ^{**} = boundary layer momentum thickness, $\int_0^\delta u/U[1-(u/U)]\,dz$

I. Introduction

THE complex phenomenon of the interaction between potential and viscous flowfields associated with airfoils has been mathematically modeled by various research groups.[1-3] The results of these computer programs show that, with the exception of drag estimation, the modeling is highly accurate for prediction of the performance of airfoils up to the onset of flow separation. References 1 and 2, however, cannot predict the post-separated boundary-layer behavior.

Several methods have been proposed to handle the post-separated boundary-layer behavior.[3-5] References 3 and 4 base their analyses on the observed constant pressure distribution in the separated regions, and introduce unbalanced sources to produce a free streamline. This modeling produces an infinitely long wake and does not simulate the details of regions of reversed flow. Reference 5 approaches the problem using an extension of boundary-layer theory to include regions of separation. These models work reasonably well when the depths of separated regions are small, but fail with large regions of separated flow.

The present experimental investigation is carried out in order to furnish a set of detailed boundary-layer characteristics under the influence of extensive separated flow conditions on a low speed airfoil. These data are intended to help the development of better mathematical models for separated flows.

II. Test Facility and Experimental Methods

The experimental investigations were carried out in the Wichita State University 2.13 ×3.05 m (7×10 ft) low speed wind tunnel fitted with a 2.13×.914 m (7×3 ft) two-dimensional insert employing a 17% thick GA(W)-1 airfoil section having a 0.61 m (24 in.) chord and a 0.914 m (36 in.) span. Details of model, supporting disks, and the surface pressure taps are given in Ref. 6. All tests were conducted at airfoil angles of attack of 10.3, 14.4, and 18.4 deg, which represent prestall, nearstall and poststall conditions, respectively. Reynolds number of the test was 2.2×10^6 based on the airfoil chord, and Mach number was 0.13. Transition was insured by employing 2.5 mm (0.1 in) wide strips of #80 carborundum grit at 5%c location on both upper and lower surfaces.[7] In the present tests, details of the flowfield were investigated on the upper surface of the model. At each angle of attack, pressure measurements were made at ten chordwise stations in order to study the behavior of the boundary layer upstream, downstream, and near the separation point on the airfoil. Details of the wake velocity and pressure distributions were obtained at four stations downstream from the trailing edge of the airfoil.

The principal instrument employed to survey the flowfield was a five-tube pressure sensing pitch-yaw probe of 3.2 mm (0.125 in.) diameter. In view of the physical dimensions of the probe, minimum height above the local surface was restricted to 2.5 mm (0.10 in.). In addition to the five-tube probe, two more probes were employed to scan the flow for heights less than 5.4 mm (0.213 in.) (Fig. 1). The first of these, a flat-tube probe, was so chosen such that the interference to the flow field was minimum. Nevertheless, at certain downstream

Received Nov. 3, 1975; revision received June 4, 1976.
Index categories: Aircraft Aerodynamics (including Component Aerodynamics); Boundary Layers and Convective Heat Transfer-Turbulent; Jets, Wakes, and Viscid-Inviscid Flow Interactions.

*Research Associate, Department of Aeronautical Engineering. Member AIAA.
†Professor, Department of Aeronautical Engineering. Associate Fellow AIAA.

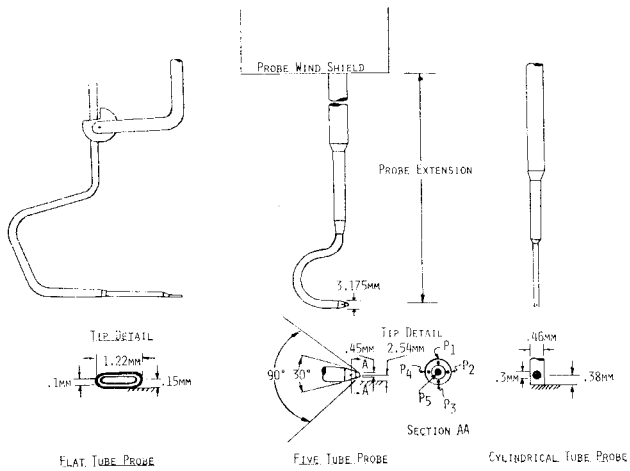

Fig. 1 Flow survey probes.

chordwise stations with shallow regions of flow reversal, the probe stem interfered with the upstream flow. Hence a cylindrical-tube probe of 0.46 mm (0.18 in.) diameter, sealed at one end, with a 0.3 mm (0.12 in.) diameter hole drilled at a height of 0.38 mm (.015 in.) from the tip was used to scan stations immediately downstream from the separation point. The probes were fixed to a mechanism which has provisions for remote traversing in the vertical axis and remote rotation of ± 180 deg about the probe axis. The traversing gear was mounted to an aluminum channel fixed to the tunnel ceiling. The probes could be positioned at any chordwise station between the leading edge and 200% chord. All the pressures were recorded by the use of unbonded strain gage differential pressure transducer of ± 17.2 kN/m^2 (± 2.5 psi) range.

Surface pressures were obtained through a system of pressure switches and transducers with digital data recorded on punch cards. Impact pressures close to the airfoil suface were measured by orienting either the flat-tube or the cylindrical tube-probe in the direction of the local flow. For these probes, velocities were computed using local surface static pressures. The majority of flowfield velocity data was acquired using the five-tube probe. The probe was initially tilted in the pitch plane to align with the local airfoil slope. The probe was then yawed as necessary to null the side-port pressure difference. Ordinarily, these adjustments amounted to ± 2 deg or less. In regions of reversal, yawing of 180 ± 40 deg was typical. Local flow upwash or downwash relative to the probe tip was determined by calibration of top and bottom pressure ports.

The five-tube probe was calibrated through a pitch angle range of ± 45 deg and with several dynamic pressures and probe extensions. Dynamic pressure and probe extension variations had negligible effects on the calibration relationships.

Corrections to the probe readings for the influence of wall were incorporated, when the probe height was within 5 diameters from the local surface. Calibration curves were extrapolated up to a maximum pitch angle of ± 50 deg.

Based on the calibration data, polynomial curve fits were employed in the data reduction program. The inputs for the data reduction program are the five pressures, probe position, and orientation in yaw. These five pressures are fed into the calibration equations to compute the local pitch angle, static pressure, total pressure, and velocity. A detailed account of the calibration procedure and the results is given by Walker.[8] While measuring the total pressure values with the flat-tube and cylindrical-tube probes, for probe positions less than 1.0 mm (0.04 in.), differential deflections of the model and the probe under aerodynamic loads resulted in erroneous probe position information.[9] Appropriate corrections for this effect have been applied to the velocity profiles.[10]

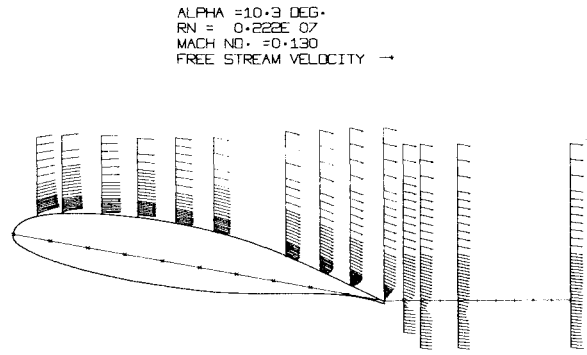

Fig. 2 Experimental velocity profile, $\alpha = 10.3$ deg.

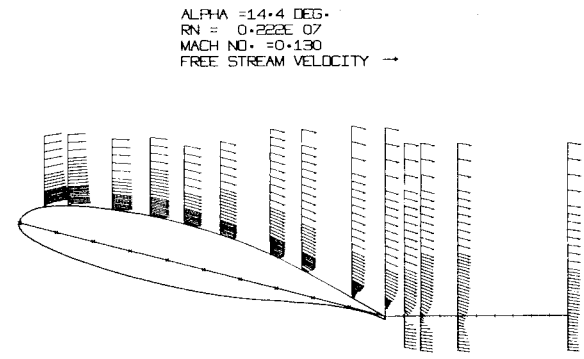

Fig. 3 Experimental velocity profile, $\alpha = 14.4$ deg.

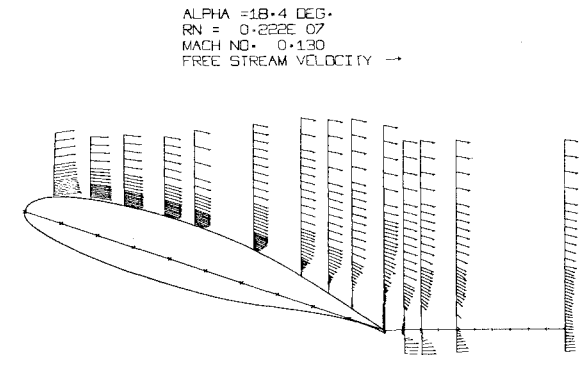

Fig. 4 Experimental velocity profile, $\alpha = 18.4$ deg.

Surface pressures, local velocities, and flow inclinations were calculated by a computer routine developed for IBM 1130 computer at WSU. Local velocity is expressed in a nondimensional form as the ratio of local to freestream velocity. Experimental velocity profiles were plotted by employing a computer plotting routine written for IBM 1130.

In addition to the surface pressure distribution, surface tufts and oil flow methods were employed to estimate the location of separation point.

Estimated accuracies for steady-state data from the five-tube probe are ± 1 deg for pitch and yaw directions and ± 2% of freestream velocity for local velocity. The flow in the turbulent separated boundary layer and the wake is basically unsteady. The instrumentation employed is heavily damped and therefore records average quantities which are subject to error depending on the local turbulence intensity.[11] Only through the use of high-response instrumentation such as hot-wire/hot-film or laser anemometry can turbulence intensity be determined accurately. Thus, it is not possible to correct the present data for unsteady-flow effects. However, the readings from the five-tube probe were generally repeatable within ± 5%, even under extreme poststall conditions.

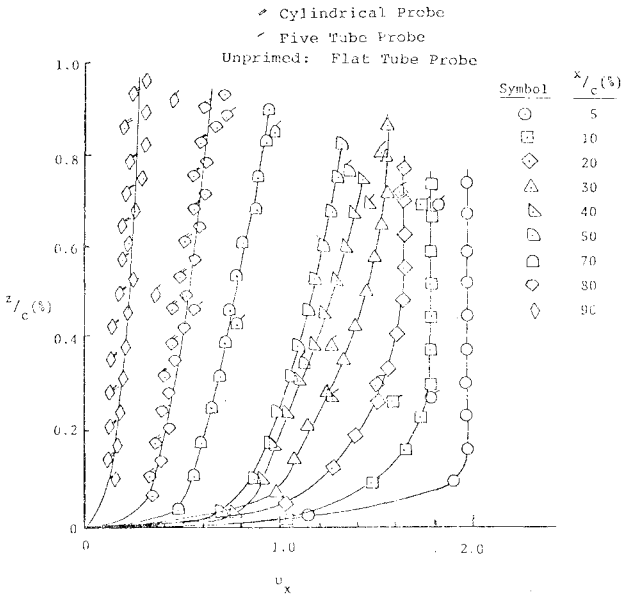

Fig. 5 Near-wall velocity profiles, $\alpha = 10.3$ deg.

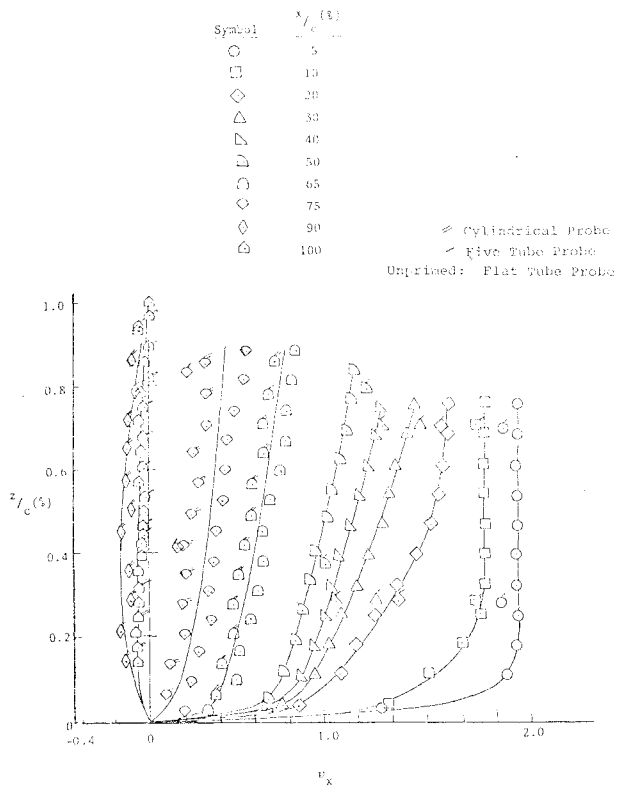

Fig. 6 Near-wall velocity profiles, $\alpha = 14.4$ deg.

III. Velocity Profiles

Computer plots of the velocity profiles at the midspan section are shown in Figs. 2-4. Velocity profiles obtained from flat-tube and cylindrical-tube probes are shown in Figs. 5-7. These profiles show that the measurements from the various probes generally agree within ±5% of the freestream velocity. Discrepancies between the probe types do not follow any consistent pattern. Perhaps the transition strip contributes to some of the larger discrepancies observed at the 5% and 10% stations. The velocity profiles at the point of separation did not in general exibit the vertical slope characteristic of separation profiles. This implies that the height above the airfoil surface in which the velocity gradient approaches zero is very small (less than about 0.05%c). This is

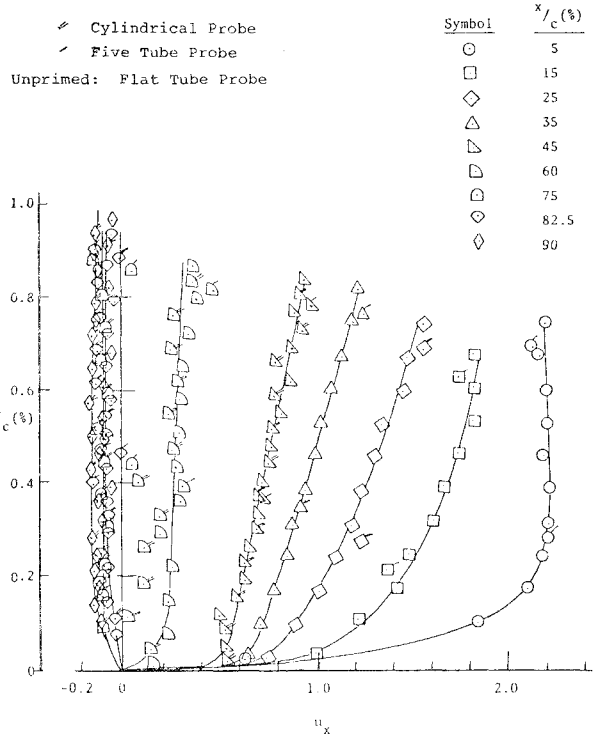

Fig. 7 Near-wall velocity profiles, $\alpha = 18.4$ deg.

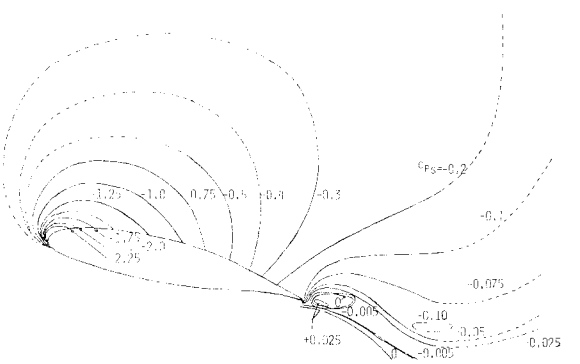

Fig. 8 Static pressure field contours, $\alpha = 10.3$ deg.

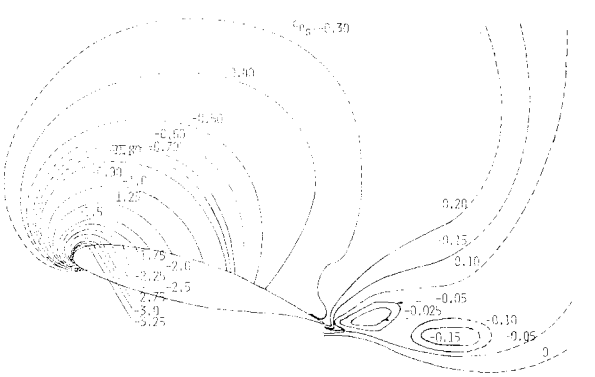

Fig. 9 Static pressure field contours, $\alpha = 14.4$ deg.

substantiated by inspecting the velocity profiles at one or two chordwise stations downstream from the separation point (for example, 90% and 100%c at 10.3 deg, 75%c at 14.4 deg, and 60% at 18.4 deg). Neither of the two probes employed could detect the reversed flow. Thus, very shallow depths of separated layer are indicated. Surface tufts, on the other hand, very clearly indicate flow reversal at these stations. Similarly, satisfactory total pressure measurements could not

be made either with flat-tube or with cylindrical-tube probes at the 100%c station for either 10.3 deg or 18.4 deg angles. This is attibuted to very low velocities with strong fluctuations around the zero velocity point at heights less than about 0.05%c above the surface. The probe interference might also be contributing to the fluctuation. In these regions the indicated dynamic pressure was negative for probe yaw directions of both 0 and 180 deg. An examination of the velocities in the wake reveals the termination of the region of flow reversal a short distance behind the trailing edge of the airfoil. The progressive longitudinal growth of the width of the wake is also seen.

IV. Overall Static Pressure Field

Static pressure contours derived from the pressure distibutions obtained at ten chordwise stations on the airfoil and four stations in the wake (x = 105.6, 110, 120, and 150%c) are shown in Figs. 8-10.

A close examination of the wake indicates a distinct high pressure plateau a short distance behind the airfoil. A relatively steep vertical pressure gradient from lower surface region to upper surface is also observed, indicating a vertical flow tendency. The velocity plots (Figs. 2-4) substantiate this tendency for upward turning of the lower surface flow.

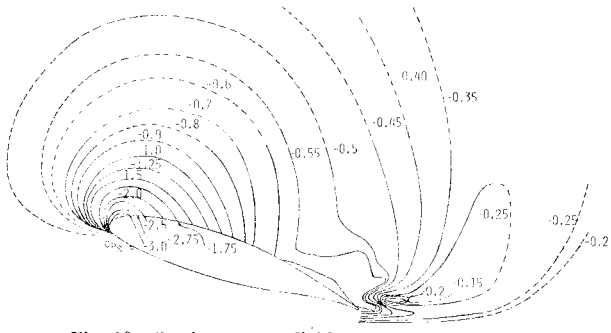

Fig. 10 Static pressure field contours, α = 18.4 deg.

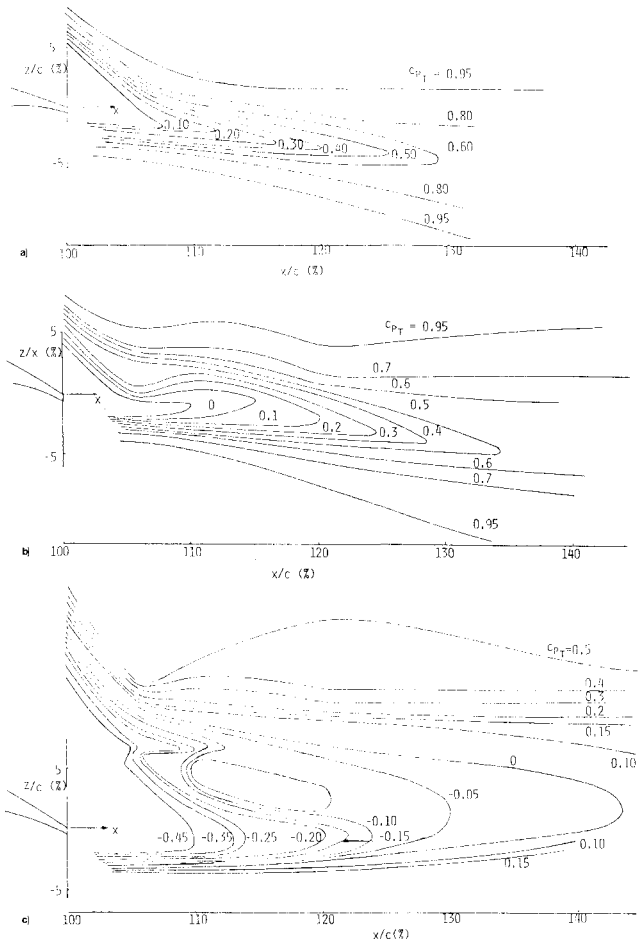

Fig. 11 Wake total pressure contours: a) α = 10.3 deg, b) α = 14.4 deg, c) α = 18.4 deg.

V. Wake Total Pressure Field

Contour plots of the wake total pressure (Fig. 11) appear to be basically different between prestall and poststall conditions. At 18.4 deg (post-stall) angle attack, two low pressure regions can be seen, whereas the 10.3 and 14.4 deg cases have only one low pressure region.

VI. Boundary-Layer Characteristics

The boundary-layer displacement thickness superimposed on the airfoil is shown in Fig. 12. The augumented surface follows the airfoil surface very closely up to the point of separation, and then diverges away with varying degrees of

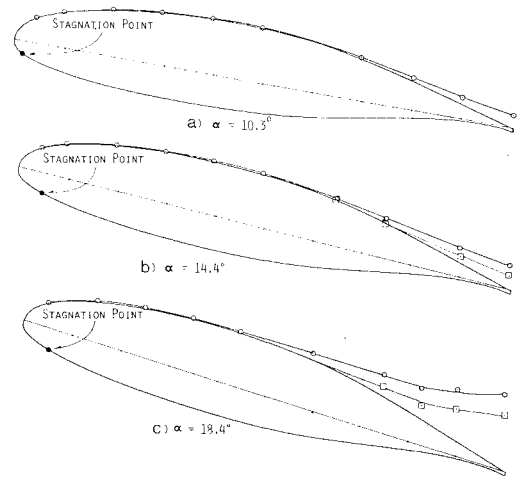

Fig. 12 Augumented airfoil profile and separation streamline. (○) Displacement thickness distribution. (□) Separtion streamline.

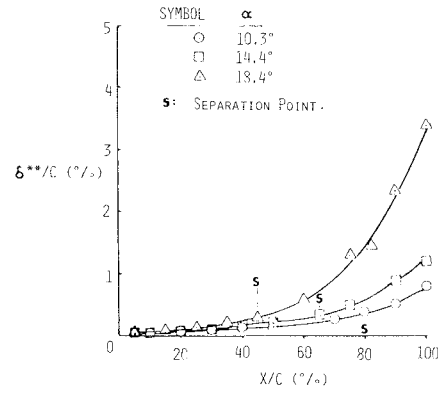

Fig. 13 Boundary-layer momentum thickness.

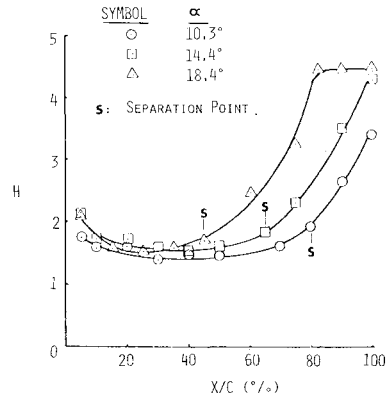

Fig. 14 Boundary-layer shape factor.

Table 1 Shape factors at separation

Angle of attack, deg	Separation point from tuft and oil flow observations, %c	Measured shape factor H
10.3	80	1.92
14.4	65	1.81
18.4	45	1.67

Table 2 Reattachment point location

Angle of attack, deg	Reattachment point, %c
10.3	103
14.4	106
18.4	117

slope depending on the depth of the separated layer. A similar trend is shown by the separation streamline, which is obtained by equation the mass flow in the reversed flow region to that of the flow in the forward direction.[12] This is shown in Figs. 12b and 12c for angles of attack of 14.4 and 18.4 deg.

The growth of momentum thickness on the airfoil (Fig. 13) indicates substantial increases between pre- and post-stall conditions. The shape factor variations at these conditions are shown in Fig. 14. The rapid growth prior to separation, typical of turbulent separated boundary layers, is clearly seen in Figs. 12–14.

It can be seen from Fig. 14 that, for the case of 18.4 deg angle of attack, the value of boundary-layer shape factor at the separation point is 1.67, which is little below the theoretical range of 1.8-2.2 ordinarily associated with separation.[13] This discrepancy is believed to be caused by the fluctuations associated with the post-stall turbulent flowfields. Shape factor values for separation points observed for 10.3 and 14.4 deg angles of attack agree very well with theoretical values (Table 1).

VII. Reattachment Point in the Wake

An examination of the wake velocity profiles (Figs. 2-4) indicates a very interesting feature. The regions of reversal in the wake terminate within a relatively short distance downstream from the trailing edge. This occurs in the region of high pressure discussed in Sec. IV. The most downstream point of reversed flow, which is characterized by a single zero velocity point in the velocity profile, is referred to as the "reattachment point." Detailed interpolation and experimentation resulted in location of reattachment points. These are tabulated in Table 2.

VIII. Characteristics of the Wake with Reversed Flow Regions

Experimental evidence from the present tests (Sec. VII) has revealed that the flow reversal region ends within a relatively short distance downstream from the airfoil trailing edge. This occurs in the region of high pressure discussed in Sec. IV. It thus appears that the mathematical models mentioned earlier which are based upon infinite wakes are not in conformity with the physical flow situation. When separation is present on the airfoil, the flow is characterized by a region of reversal near the wall, with a shear layer extending outward to the freestream. This shear layer entrains mass from the region of reversal and carries it outward and downstream. Since the outer shear layer source of entrainment energy is essentially infinite, the region of reversal must end at a finite distance downstream from the trailing edge.

The presently proposed picture of the separated wake is analogous to the well-known "near-wake" and "far-wake" regions commonly used to describe supersonic wake flows.[14] The near wake is dominated by the characteristic recirculating flow resulting from the separated shear layer. In the far-wake region, on the other hand, the rotational velocity field diffuses, forming a free-shear region characterized by small scale turbulence. Mathematical modeling and analysis of the wake characteristics including the far wake may provide a theoretical approach to the very important matter of drag prediction.

IX. Conclusions

Experimental velocity profiles, flow inclinations, and static pressure distributions have been obtained for the GA(W)-1 airfoil upper surface and wake at typical pre-and post-stall angle of attack conditions. The data include reversed flow regions of separated boundary layers. Integrations of velocity profiles to obtain displacement thickness, momentum thickness, and the separation streamline show that all of these parameters exhibit a rather steep diverging trend from the separation point to the airfoil trailing edge. The present test reveal that the region of reversed flow associated with separation terminates at a reattachment point which is located a short distance downstream from the airfoil trailing edge.

It is hoped that these data will clarify some doubts and deficiencies associated with the current computational techniques, and that more effective and accurate mathematical models for separated flows will emerge.

Acknowledgment

This research was sponsored by NASA Langley Research Center under NGR 17-003-021.

References

[1] Liebeck, R.H. "A Class of Airfoils Designed for High Lift in Incompressible Flow," *Journal of Aircraft*, Vol. 10, Oct. 1973, pp. 610-617.

[2] Stevens, W.A., Goradia, S.H., and Braden, J.A., "Mathematical Model for Two-Dimensional Multi-Component Airfoil in Viscous Flow," NASA CR-1843, July 1971.

[3] Bhateley, I.C. and McWhirter, J.W., "Development of Theoretical Method for Two-Dimensional Multi-element Airfoil Analysis and Design, Part 1-Viscous Flow Analysis Method," Air Force Flight Dynamics Lab, Wright Patterson AFB, Ohio, AFFDL-TR-73-96, Aug. 1972.

[4] Hahn, M. Rubbert, P.E., and Mahal, A.S., "Evaluation of Separation Criteria and Their Applications to Separated Flow Analysis," Air Force Flight Dyanmics Lab, Wright Patterson AFB, Ohio, AFFDL-TR-72-145, Jan. 1973.

[5] Kuhn, G.D. and Nielsen, J.N., "Prediction of Turbulent Separated Boundary Layer," *AIAA Journal*, Vol. 12, July 1974, pp. 881-882.

[6] Wentz, W.H. Jr. and Seetharam, H.C., "Developement of a Fowler Flap System for A High Performance General Aviation Airfoil," NASA CR-2443, Dec. 1974.

[7] Braslow, A.L. and Knox, E.C., "Simplified Method for Determination of Critical Height of Distributed Roughness Particles for Boundary Layer Transition at Mach Numbers from 0-5," NACA TN-4363, 1958.

[8] Walker, J.K., "Calibration of a Five-Tube Probe," Wichita State University, Wichita, Kan., WSU AR 74-1, April 1974.

[9] Peterson, J.B., Jr, "Boundary-Layer Velocity Profiles Downstream of Three-Dimensional Transition Trips on a Flat-Plate at Mach 3 and 4," NASA TN-D-5523, 1969.

[10] Seetharam, H.C. and Wentz, W.H., Jr, "Experimental Studies of Flow Separation and Stalling on a Two-Dimensional Airfoil at Low Speeds," NASA CR-2560, July 1975.

[11] Gault, D.E., "An Investigation at Low Speed of the Flow over a Simulated Flat Plate at Small Angles of Attack using Pitot-Static and Hot-Wire Probes," NACA TN-3876, March 1957.

[12] Seetharam, H.C., "Experimental Investigation of Separated Flow Fields on an Airfoil at Subsonic Speeds," Ph.D. Thesis, Wichita State University and University of Kansas Joint Doctoral Program, March 1975.

[13] Schlichting, H. *Boundary Layer Theory*, McGraw-Hill Co., New York, 4th Ed., 1962.

[14] Modi, V.J. and Dikshit, A.K "Near Wakes of Elliptic Cylinders in Subcritical Flow," *AIAA Journal*, Vol. 13, April 1975, pp. 490-497.